PHYSICAL REVIEW A **70**, 061804(R) (2004)

Resonant four-wave mixing with slow light

Hoonsoo Kang, Gessler Hernandez, and Yifu Zhu
Department of Physics, Florida International University, Miami, Florida 33199, USA
(Received 8 June 2004; published 15 December 2004)

Electromagnetically induced transparency in a four-level atomic system suppresses the linear susceptibility and enhances the nonlinear susceptibilities, which leads to the resonantly enhanced slow-light four-wave mixing at low light intensities. We report an experimental observation of such resonant four-wave mixing in cold Rb atoms.

DOI: 10.1103/PhysRevA.70.061804 PACS number(s): 42.50.Gy, 42.65.−k, 32.80.−t

Electromagnetically induced transparency (EIT) has been used recently to obtain vanishing linear absorption and large nonlinear susceptibilities, as well as slow light speed in an absorbing medium [1]. It has been shown that it is possible to study nonlinear optics near the resonant frequencies of the atomic transitions in an EIT medium at low light levels down to single photons [2]. This opens up possibilities of applying the EIT technique to explore quantum nonlinear optics and quantum information processing [3].

EIT manifested nonlinear optical phenomena have been a subject of many recent studies. In particular, four-wave mixing (FWM) in three-level and four-level EIT systems with a variety of laser coupling schemes has been studied by various groups in recent years [4–15]. So far, the experimental studies of FWM in EIT media are largely carried out in vapor cells or solids in which inhomogeneous broadening is dominant and the pump light intensities applied are typically above the atomic saturation intensities. In a four-level system, the added pump field necessary for the FWM process modifies the EIT line profile. When the pump intensity approaches the saturation level, the steep normal dispersion for the weak probe light disappears and the EIT medium ceases to support the slow photon propagation. Theoretical studies predict that the EIT manifested slow photons and the enhanced nonlinearity greatly increase the FWM efficiency and render the efficient FWM observable at low light intensities [2,15]. Here we report an experimental study of four-wave mixing resonantly enhanced by EIT in a four-level system realized with cold Rb atoms. Our experiment was done at the pump and probe intensities below the saturation levels, which ensures the slow group velocities for the probe light and the generated signal light. We observed directly the slow light propagation and obtained a high FWM efficiency ~10%.

Consider a four-level Rb system depicted in Fig. 1(a) (the coupled ^{87}Rb D_1 transition lines form several separate four-level channels and to a good approximation, can be treated as an effective four-level EIT system). A coupling laser driving the transition $|2\rangle-|3\rangle$ with Rabi frequency Ω_c and a weak probe laser driving the transition $|1\rangle-|3\rangle$ with Rabi frequency Ω_p form the standard Λ-type EIT configuration. A pump laser drives the transition $|2\rangle-|4\rangle$ with Rabi frequency Ω and facilitates a nondegenerate FWM process, $|1\rangle\rightarrow|3\rangle\rightarrow|2\rangle\rightarrow|4\rangle\rightarrow|1\rangle$, which results in the emission of photons with a wave vector $\mathbf{k}_s$ at the frequency ω_s. The required phase-matching condition is given by $\mathbf{k}_p-\mathbf{k}_c=\mathbf{k}_s-\mathbf{k}$ [$\mathbf{k}_j$ ($j=p$ and c) is the wave vector of the input probe (p) and the coupling (c) fields, respectively, and $\mathbf{k}$ is the wave vector of the pump field]. In our experimental arrangement of the *backward* FWM configuration [Fig. 1(b)], $\mathbf{k}=-\mathbf{k}_c$, the phase-matching condition reduces to $\mathbf{k}_s=2\mathbf{k}+\mathbf{k}_p$, which is satisfied with $\theta p\approx\theta s=\theta\approx 0.34°$ for the Rb system.

Without the pump laser, the Rb system exhibits the standard Λ-type EIT and the probe-laser pulse propagates with a slow group velocity. When the pump laser is added, the EIT line profile is modified, which leads to the enhanced third-order nonlinearity [16–19]. For $\Omega_c\gg\Omega_p$ and $\Delta_c=\Delta=0$ [$\Delta_c(\Delta)$ is the frequency detuning of the coupling (pump) laser], the group velocity of the probe light is given by

$$V_g=\frac{c}{1+\left.\dfrac{\omega_p}{2}\dfrac{\partial\chi(\omega_p)}{\partial\omega_p}\right|_{\Delta p=0}}, \tag{1}$$

where $\chi(\omega_p)$ is the atomic susceptibility at the probe frequency ω_p, $\Delta_p=\omega_p-\omega_{13}$ is the probe frequency detuning, c is the light speed in vacuum, and

$$\left.\frac{\partial\chi(\omega_p)}{\partial\omega_p}\right|_{\Delta_p=0}=\frac{4K(|\Omega_c|^2\Gamma_4{}^2-|\Omega|^4-|\Omega|^2(|\Omega_c|^2+2\Gamma_2\Gamma_4)-(\Gamma_2\Gamma_4)^2)}{(\Gamma_3|\Omega|^2+\Gamma_4|\Omega_c|^2+\Gamma_2\Gamma_3\Gamma_4)^2}. \tag{2}$$

Here $K=N|\mu_{13}|^2/(3V\varepsilon_0\hbar)$ and $\Gamma_2(\ll\Gamma_3)$ is the decay rate of the $|2\rangle-|1\rangle$ coherence. When $\partial\chi(\omega_p)/\partial\omega_p=0$, Eq. (2) results in a critical value Ω_0 of the pump Rabi frequency Ω,

$$|\Omega_0|^2\equiv\frac{\sqrt{|\Omega_c|^4+4|\Omega_c|^2(\Gamma_4{}^2+\Gamma_2\Gamma_4)}-|\Omega_c|^2-2\Gamma_2\Gamma_4}{2}<\Gamma_4{}^2. \tag{3}$$

When $|\Omega|^2=\Omega_0|^2$, $V_g=c$; when $|\Omega|^2<\Omega_0|^2$, the EIT medium exhibits normal dispersion and $V_g<c$; and when $|\Omega|^2>\Omega_0|^2$, the EIT medium exhibits anamalous dispersion and $V_g>c$ or become negative ($V_g<0$) [20]. Therefore, with a weak pump laser ($|\Omega|<|\Omega_0|$), the four-level system exhibits vanishing linear absorption and greatly enhanced nonlinear susceptibilities while preserving the normal slope of the probe dispersion, which enables the FWM process to pro-

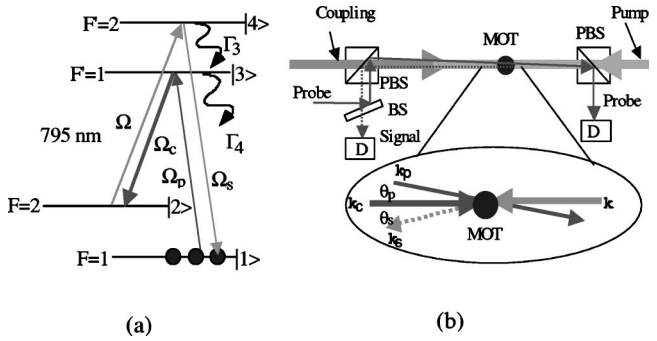

FIG. 1. (a) FWM coupling scheme of the four-level ^{87}Rb atoms. $\Gamma_3(\Gamma_4)$ is the spontaneous decay rate ($\Gamma_3 \approx \Gamma_4 = 2\pi \times 5.4 \times 10^6\ s^{-1}$). (b) Simplified experimental set up. BS, beam splitter ($T=92\%$, $R=8\%$); PBS, polarizing beam splitter; *D*, photodetector.

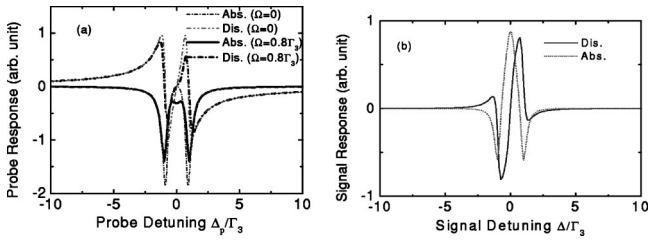

FIG. 2. (a) Calculated probe response vs the probe frequency detuning in the four-level EIT system (all other lasers are on resonance). (b) Calculated signal response vs the signal frequency detuning in the four-level EIT system (all other lasers are on resonance). The parameters are $\Omega_c = 1.8\Gamma_3$, $\Omega = 0.8\Gamma_3$, $\Omega_p = 0.2\Gamma_3$, and $\Omega_s = 0.02\Gamma_3$. For the absorption curves, values $>0(<0)$ indicate gain (absorption). Note that both the probe and the signal see the steep normal dispersion near their respective resonant frequencies, which results in slow group velocities for both the probe pulse and the generated signal pulse.

ceed with slow light speed for the probe photons. When the Rabi frequency Ω_s of the generated FWM field is weak ($|\Omega_s| < |\Omega||\Omega_p|/\Omega_c|$) [21], the signal photons also propagate with a reduced group velocity. This is the regime where the FWM produces the signal photons with a high efficiency, and may lead to quantum entanglement between the probe photons and signal photons [22]. To provide the physical insight for the slow photon propagation, we calculated the probe response and the signal response (single atom response and excluding propagation effects) in the four-level EIT system by assuming that the generated FWM field is weaker than the probe field ($|\Omega_s| < |\Omega_p|$). The calculated results are plotted in Fig. 2. Figure 2(a) presents the probe absorption and dispersion versus the probe frequency detuning. Without the pump laser, the probe response exhibits the usual EIT line profile with vanishing absorption at $\Delta p = 0$ and the steep normal dispersion near $\Delta p = 0$. With a weak pump laser, the probe laser experiences the nonlinear absorption (with the reduced EIT transparency window) at $\Delta p = 0$ [16–19] while still seeing the normal dispersion near the resonance. Figure 2(b) presents the signal gain and dispersion profile versus the signal frequency detuning (the other three fields are all on their respective resonances). It shows that the FWM field is amplified in the EIT system with the gain peaked at the resonance and the signal dispersion also has a steep normal shape. Therefore, for the FWM process in the four-level EIT system at low pump intensities, both the probe light and the generated signal light propagate with slow group velocities.

Our experiment is done with cold ^{87}Rb atoms confined in a magneto-optical trap (MOT). A tapered-amplifier diode laser (TA-100, Tuioptics) with output power $\sim$400 mW is used as the cooling laser. An extended-cavity diode laser with an output power of $\sim$30 mW is used as the repump laser. The diameter of the trapping laser beams and the repumping laser beam is $\sim$2.5 cm. The ^{87}Rb atoms are trapped with the cooling laser and the repump laser tuned to the D_2 transitions. The trapped ^{87}Rb atom cloud is $\sim$2 mm in diameter and contains $\sim 10^9$ atoms. A simplified experimental scheme is depicted in Fig. 1(b). The coupling field driving the $D_1F = 2 - F' = 1$ transition is provided by a third extended-cavity diode laser with a beam diameter $\sim$5 mm and output power $\sim$20 mW. A fourth extended-cavity diode laser driving the $D_1F = 2 - F' = 2$ transition provides the pump laser beam with a beam diameter $\sim$5 mm. The probe laser driving the $D_1F = 1 - F' = 1$ transition is provided by a fifth extended-cavity diode laser with a beam diameter $\sim$0.5 mm. The probe laser, the coupling laser, and the pump laser are overlapped with the trapped Rb cloud as shown in Fig. 1(b). The coupling laser and the pump laser are linearly polarized parallel with each other, which is perpendicular to the linearly polarized probe laser. Two polarizing beam splitters are used to combine and separate the probe light, the coupling light, the pump light, and the generated FWM signal light. The small angle $\theta p \approx \theta s = \vartheta(\sim 0.34°)$ nearly satisfies the phase-matching condition and also ensures that the transmitted probe beam and the generated signal light are spatially separated from the residual pump and coupling beams at the detector positions. The transmitted probe light and the generated FWM signal light (with the same linear polarization as the probe light) are collected by two photodiode detectors. The spatial position of the signal detector is carefully aligned and optimized for the generated signal that is observed to depend on three laser beams simultaneously.

The experiment is run in a sequential mode with a repetition rate of 5 Hz. All lasers are turned on or off by acousto-optic modulators (AOM) according to the time sequence described below. For each period of 200 ms, $\sim$198 ms is used for cooling and trapping of the Rb atoms, during which the trap laser and the repump laser are turned on by two separate AOMs while the coupling laser, the probe laser, and the pump laser are off. The time for the FWM measurement lasts $\sim$2 ms, during which the trap laser and the repump laser are turned off, and the coupling laser and the pump laser are turned on. 100 μs after the coupling laser and the pump laser are turned on, the probe-laser pulse is turned on. The generated signal pulse and the transmitted probe pulse are then recorded versus the time.

Figure 3 shows the measured probe transmission spectrum and the FWM emission spectrum versus the probe frequency detuning Δ_p. For these measurements, the probe laser is turned on and off at the same time as the coupling and the pump lasers (with the same 2-ms duration). After a 100-μs delay, the probe-laser frequency is scanned across the D_1F

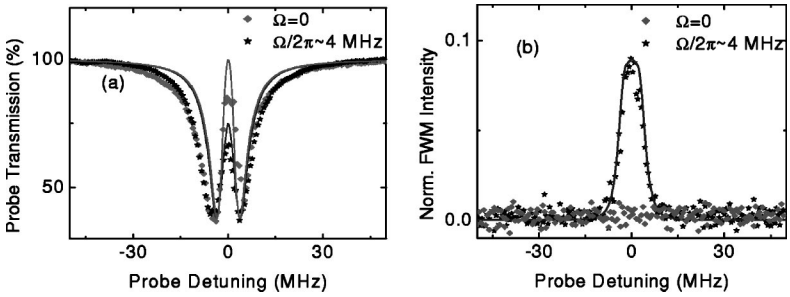

FIG. 3. (a) Measured (dots) and calculated (solid lines) probe transmission, and (b) measured (dots) and calculated (solid lines) FWM intensity (normalized relative to the probe intensity) vs the probe frequency detuning Δ_p. The coupling laser and the pump laser are on resonance ($\Delta_c=\Delta=0$). $\Omega_c/2\pi\approx 8$ MHz, $\Omega_p/2\pi \approx 0.4$ MHz, and $\Omega/2\pi\approx 4$ MHz.

$=2\rightarrow F'=1$ transition, and the probe transmission and the FWM emission are recorded versus the probe detuning. The dots in Fig. 3 are the experimental data and the solid lines are the numerical calculations of the coupled Maxwell equations for the four-level EIT system (under the slowly varying amplitude approximation). Figure 3 shows that without the pump laser, the observed probe transmission exhibits a deep EIT window and no signal from the FWM process is observed. When the weak pump laser is present, the transmission spectrum shows a large increase of the probe attenuation near the resonance, demonstrating the EIT enhanced nonlinear absorption [Fig. 3(a)] [16–19]. The measured FWM emission spectrum is plotted in Fig. 3(b), which exhibits a single peak coinciding with the EIT window. Under our experimental conditions, the observed FWM efficiency η defined as the ratio of the FWM signal intensity I_F and probe intensityI_p, I_F/I_p, is about 10%. It has been shown theoretically [15] that under the conditions of strong-coupling field and pump field in an optically dense medium, the generated FWM intensity in the *forward* FWM configuration is sufficiently high to reach the regime where $|\Omega_s|\approx|\Omega||\Omega_p|/|\Omega_c|$, then the three-photon destructive interference limits the FWM efficiency at the resonance. In such a regime, the FWM emission is maximized with the detuned probe and coupling lasers [15]. Our experiment is done in the *backward* FWM configuration with weak pump and moderate coupling lasers, and the FWM efficiency is limited further by the finite number of cold atoms in the MOT. The generated FWM intensity is weak ($|\Omega_s|<|\Omega||\Omega_p|/|\Omega_c|$) so the three-photon destructive interference is not dominant, and the observed FWM is peaked near the resonant EIT condition as shown in Fig. 3.

Next, we present the FWM measurements with a pulsed probe field, in which the frequencies of the three lasers are fixed on resonance with their respective transitions. The experimental measurements for an input probe pulse of $\tau \approx 0.6$ μs duration are plotted in Fig. 4. We observed that within the experimental uncertainty, the measured signal pulse [Fig. 4(b)] matches the temporal shape of the input probe pulse. The pulse duration of ~ 0.6 μs in our experiment is much larger than the relaxation time ($1/\Gamma_3\approx 1/\Gamma_4 =29.4$ ns) of the atomic system. Therefore, the atomic system is in the adiabatic steady state and the generated signal pulse follows the rise and fall of the incident probe pulse. We calculate that under our experimental conditions ($\Omega_c/2\pi \approx 9$ MHz, and $\Omega/2\pi\approx 4$ MHz), the probe pulse travels with a group velocity $\sim 10^5$ m/s in the four-level EIT medium and is delayed by ~ 16 ns relative to the reference probe pulse propagating in vacuum. The calculations agree with the measurements shown in Fig. 4(a) for the two lower curves corresponding to the probe pulse transmitted through the three-level Λ-type EIT medium (curve 2, no pump laser) and the probe pulse passing through the four-level EIT medium modified by the weak pump laser (curve 3), respectively. By fitting the transmitted probe pulse with a Gaussian shape, $I =I_0\exp[-2(t-\Delta t)^2/\tau^2]$, and taking the average for ten measurements, we derive that the probe pulse propagating through the three-level EIT medium (without the pump laser) is delayed by 25 ± 9 ns relative to the reference probe pulse and the probe pulse propagating through the four-level EIT medium during the FWM process (with the pump laser) is delayed by 17 ± 10 ns. Overall, the measurements show that the transmitted probe pulses maintain nearly the same temporal profile and the pulse distortion is small. We also observed that when the pump Rabi frequency increases to $\Omega/2\pi>6$ MHz, no time delay between the transmitted probe pulse and the reference probe pulse is observed, verifying that the slow photon FWM only occurs at the weak pump intensities.

It is instructive to study the dependence of the FWM efficiency and the probe group velocity on the coupling Rabi frequency Ω_c. Figure 5(a) plots the group velocity of the probe light versus the coupling Rabi frequency Ω_c calculated from Eq. (1) and shows that with a fixed weak pump, when $|\Omega_c|^2<|\Omega_{c0}|^2$, $V_g>c$; when $|\Omega_c|^2>|\Omega_{c0}|^2$, $V_g<c$. The probe group velocity reaches the minimum value for a moderate Ω_c value, after which the group velocity increases slowly with the increasing Ω_c. Figure 5(b) shows the dependence of the FWM signal intensity versus Ω_c. The FWM signal intensity

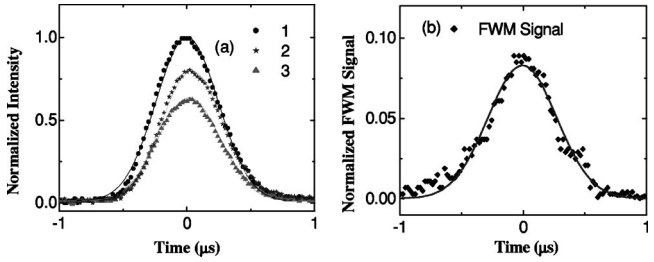

FIG. 4. (a) Measured probe transmission and (b) measured FWM intensity vs time for an incident probe pulse of ~ 0.6 μs duration. In (a), top curve 1 is the reference probe pulse; curve 2 is the transmitted probe pulse with EIT only (without the pump laser); curve 3 is the transmitted probe pulse with the EIT modified by the pump laser. The dots are the experimental data and the solid lines are the Gaussian pulse fits. The scale is normalized relative to the reference probe. The experimental parameters are $\Omega_c/2\pi \approx 9$ MHz, $\Omega_p/2\pi\approx 0.4$ MHz, $\Omega/2\pi\approx 3$ MHz, and $\Delta_p=\Delta_c=\Delta=0$.

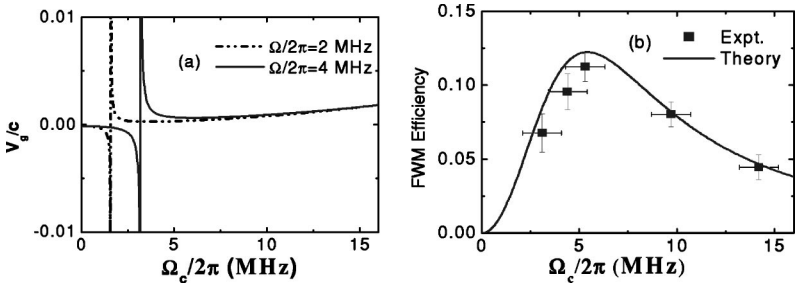

FIG. 5. (a) The calculated group velocity of the probe light and (b) the FWM efficiency vs the coupling Rabi frequency Ω_c. The dots (solid lines) are the experimental data (theoretical calculations). The experimental parameters are $\Omega/2\pi \approx 4$ MHz, $\Omega_p/2\pi \approx 0.4$ MHz.

first increases with Ω_c, reaches the maximum near $\Omega_c/2\pi \approx 5$ MHz, and then decreases with the further increase of Ω_c. Figure 5 shows that the slower group velocity correlates qualitatively with the larger FWM efficiency, which is related to the EIT width. Since the EIT width increases with Ω_c, broadening of the EIT width lowers the FWM efficiency and increases the group velocity.

In conclusion, the EIT enhancement of the nonlinear susceptibilities and suppression of the linear susceptibility enable us to observe the efficient nondegenerate FWM at low light intensities and slow light conditions. We have shown that both the probe light and the generated signal light propagate at slow group velocities, which occurs only at the weak pump intensity conditions. With an improved experimental set up and tight focusing of the probe beam, it may be possible to study the slow light FWM at single-photon levels, and explore its application in the generation of photon correlation and quantum entanglement [22–24].

This work is supported by the National Science Foundation.

[1] S. E. Harris, Phys. Today **50**, 36 (1997).
[2] S. E. Harris and L. V. Hau, Phys. Rev. Lett. **82**, 4611 (1999).
[3] M. D. Lukin and A. Imamoglu, Nature (London) **413**, 273 (2001).
[4] K. Hakuta, L. Marmet, and B. P. Stoicheff, Phys. Rev. Lett. **66**, 596 (1991); Q. J. Liang, M. Katsuragawa, F. Le Kien, and K. Hakuta, *ibid.* **85**, 2474(2000).
[5] M. Jain, H. Xia, G. Y. Yin, A. J. Merriam, and S. E. Harris, Phys. Rev. Lett. **77**, 4326 (1996).
[6] M. Fleischhauer and T. Richter, Phys. Rev. A **51**, 2430 (1995); M. Fleischhauer, A. B. Matsko, and M. O. Scully, *ibid.* **62**, 013808 (2002); M. D. Lukin, A. B. Matsko, M. Fleischhauer, and M. O. Scully, Phys. Rev. Lett. **82**, 1847 (1999); S. F. Yelin, V. A. Sautenkov, M. M. Kash, G. R. Weltch, and M. D. Lukin, Phys. Rev. A **68**, 063801 (2003).
[7] P. R. Hemmer *et al.*, Opt. Lett. **20**, 982 (1995); T. T. Grove *et al.*, *ibid.* **22**, 769 (1997); B. S. Ham, M. S. Shahriar, and P. R. Hemmer, *ibid.* **24**, 86 (1999).
[8] Y. Li and M. Xiao, Opt. Lett. **21**, 1064 (1996); B. L. Lu, W. H. Burkett, and M. Xiao, *ibid.* **23**, 804 (1998).
[9] W Harshawardhan and G. S. Agarwal, Phys. Rev. A **58**, 598 (1998).
[10] A. S. Zibrov, M. D. Lukin, and M. O. Scully, Phys. Rev. Lett. **83**, 4049 (1999); A. S. Zibrov, M. D. Lukin, L. Hollberg, and M. O. Scully, Phys. Rev. A **65**, 051801 (2002); A. S. Zibrov, A. B. Matsko, and M. O. Scully, Phys. Rev. Lett. **89**, 103601 (2002); M. D. Lukin, P. R. Hemmer, and M. O. Scully, Adv. At., Mol., Opt. Phys. **42**, 347 (2000), and references therein.
[11] C. Dorman, I. Kucukkara, J. P. Marangos, Phys. Rev. A **61**, 013802 (2000); J. P. Marangos, J. Mod. Opt. **45**, 471 (1998); E. A. Korsunsky, T. Halfmann, J. P. Marangos, and K. Bergmann, Eur. Phys. J. D **23**, 167 (2003); J. C. Petch, C. H. Keitel, P. L. Knight, and J. P. Marangos, Phys. Rev. A **53**, 543 (1996).
[12] C. H. Keitel, Phys. Rev. A **57**, 1412 (1998).
[13] M. T. Johnsson and M. Fleischhauer, Phys. Rev. A **66**, 043808 (2002).
[14] A. K. Popov and A. S. Bayev, Phys. Rev. A **62**, 025801 (2000).
[15] L. Deng and M. G. Payne, Phys. Rev. A **65**, 063806 (2002).
[16] H. Schmidt and A. Imamoglu, Opt. Lett. **21**, 1936 (1996).
[17] S. E. Harris and Y. Yamamoto, Phys. Rev. Lett. **81**, 3611 (1998).
[18] M. Yan, E. Rickey, and Y. Zhu, Opt. Lett. **26**, 548 (2001).
[19] D. A. Braje, V. Balic, G. Y. Yin, and S. E. Harris, Phys. Rev. A **68**, 041801(R) (2003).
[20] H. Kang, G. Hernandez, and Y. Zhu, Phys. Rev. A **70**, 011801(R) (2004).
[21] L. Deng and M. G. Payne, Phys. Rev. A **68**, 051801(R) (2003).
[22] M. G. Payne and L. Deng, Phys. Rev. Lett. **91**, 123602 (2003).
[23] A. Kuzmich *et al.*, Nature (London) **423**, 731 (2003).
[24] C. H. Van der Wal *et al.*, Science **301**, 196 (2003).